A Quadratic Linked Plate Element With an Exact Thin Plate Limit *

R.L. Taylor† and S. Govindjee‡

Department of Civil and Environmental Engineering
University of California at Berkeley
Berkeley, California

November 18, 2002

Abstract

In this report we detail the development of a 6 node triangular plate element suitable for use in the simulation of anisotropic materials that generate membrane-shear coupling. Our canonical example of such a material is single crystal Silicon in the [111] wafer orientation. The plate developed utilizes quadratic fields to take advantage of the good convergence properties of quadratic elements in linear problems. Further we utilize linked interpolations to produce an element with an exact thin plate limit. Thus the proposed element is useful for both thin and thick plates. Bubble modes are added to the element to give it full convergence properties that one would expect from a quadratic type element. Convergence studies are presented at the end utilizing both isotropic and anisotropic plates. An appendix is provided with programing details in addition to an appendix detailing the anisotropic properties of Silicon plates.

1 INTRODUCTION

The development of computational models for plate bending problems dates from the earliest days of structural analysis and the literature is too extensive

*Technical Report: UCB/SEMM-2002/10

†Professor in the Graduate School, e-mail: rlt@ce.berkeley.edu

‡Associate Professor, e-mail: sanjay@ce.berkeley.edu

to fully cite here. A rather late development for such analyses; however, is one in which a linking between transverse displacements and rotation is used with the Reissner-Mindlin from of a shear deformable theory. This was introduced for elements which started from linear and bi-linear interpolations of displacement fields by Zienkiewicz *et al.* [1, 2] and Taylor & Auricchio [3]. These were extended to permit solutions at the thin plate limit by Auricchio & Taylor [4, 5]. Earlier an element starting from quadratic order interpolations was introduced by Zienkiewicz & Lefebvre [6] and was considered to be convergent and fully robust. Recently, this element was extended by Auricchio & Lovadina to include linked interpolation [7]. They also extended the analysis of Lovadina [8] to show that adding additional internal modes resulted in an element that exhibits optimal rates of convergence while remaining fully robust at the thin plate limit. Here we extend this past work to treat the case of coupled membrane-transverse shear effects due to material anistoropy with an eye towards the simulation of single crystal silicon plates in MEMS design.

2 Reissner-Mindlin Plate Theory

In the Reissner-Mindlin theory of plates the displacement field is expressed by the transverse displacement and two rotations parameters for a line initially normal to the reference surface (Fig. 1). Accordingly we let the displacement field be represented by

$$\begin{aligned} u_x(x,y,z) &= u(x,y) + z\,\phi_x(x,y) \\ u_y(x,y,z) &= v(x,y) + z\,\phi_y(x,y) \\ u_z(x,y,z) &= w(x,y) \end{aligned} \tag{1}$$

where x, y define the plane of the plate; z is a direction normal to the plane; u, v, w are displacements at a reference surface of the plate ($z = 0$); and ϕ_x, ϕ_y represent the director rotation in the directions x, y, respectively. Later the director rotation, $\boldsymbol{\phi}$, will be expressed in terms of angle rotations about the axes, $\boldsymbol{\theta}$, using the transformation

$$\left\{ \begin{array}{c} \theta_x \\ \theta_y \end{array} \right\} = \left[\begin{array}{cc} 0 & -1 \\ 1 & 0 \end{array} \right] \left\{ \begin{array}{c} \phi_x \\ \phi_y \end{array} \right\} \quad \text{or} \quad \left\{ \begin{array}{c} \phi_x \\ \phi_y \end{array} \right\} = \left[\begin{array}{cc} 0 & 1 \\ -1 & 0 \end{array} \right] \left\{ \begin{array}{c} \theta_x \\ \theta_y \end{array} \right\} \quad . \tag{2}$$

Using the usual small displacement theory for plates we then obtain the

non-zero in-plane strains:

$$\begin{aligned} \epsilon_{xx} &= \frac{\partial u}{\partial x} + z\,\frac{\partial \phi_x}{\partial x} \\ \epsilon_{yy} &= \frac{\partial v}{\partial y} + z\,\frac{\partial \phi_y}{\partial y} \\ \gamma_{xy} &= \frac{\partial u}{\partial y} + \frac{\partial v}{\partial x} + z\,(\frac{\partial \phi_x}{\partial y} + \frac{\partial \phi_y}{\partial x}) \end{aligned} \tag{3}$$

and the transverse shearing strains

$$\begin{aligned} \gamma_{yz} &= \frac{\partial w}{\partial y} + \phi_y \\ \gamma_{zx} &= \frac{\partial w}{\partial x} + \phi_x \quad . \end{aligned} \tag{4}$$

Force resultants in the plate are defined by integrating the stresses over

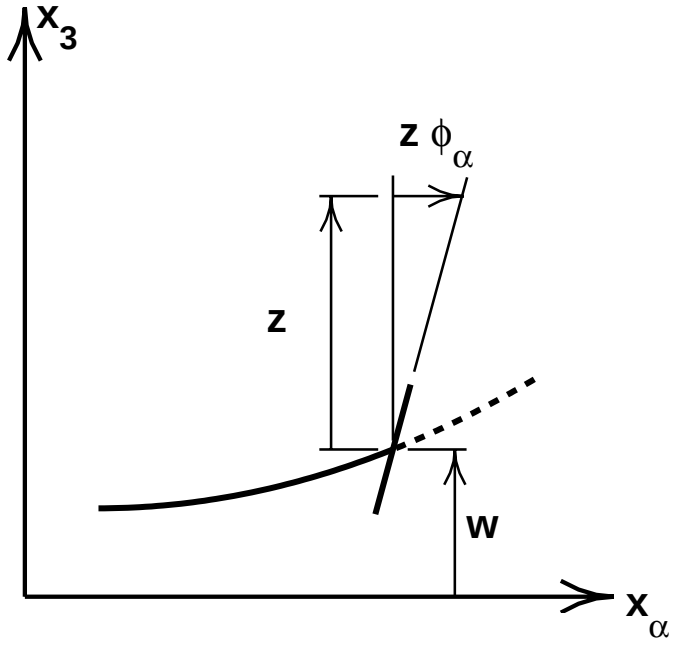

Figure 1: Displacement parameters for plate

the thickness, h. Accordingly, for the in-plane resultants we obtain

$$\begin{aligned} N_{xx} &= \int_h \sigma_{xx}\,\mathrm{d}z\ , & M_{xx} &= \int_h z\,\sigma_{xx}\,\mathrm{d}z \\ N_{yy} &= \int_h \sigma_{yy}\,\mathrm{d}z\ , & M_{yy} &= \int_h z\,\sigma_{yy}\,\mathrm{d}z \\ N_{xy} &= \int_h \tau_{xy}\,\mathrm{d}z = N_{yx}\ , & M_{xy} &= \int_h z\,\tau_{xy}\,\mathrm{d}z = M_{yx} \end{aligned} \tag{5}$$

where N_{ij} are force resultants and M_{ij} are moment resultants, each per unit length of plate. Similarly, the transverse shearing forces are given by

$$\begin{aligned} Q_y &= \int_h \tau_{yz}\,\mathrm{d}z \\ Q_x &= \int_h \tau_{zx}\,\mathrm{d}z\ \ . \end{aligned} \tag{6}$$

The equilibrium equations for the plate may be obtained by integrating through the thickness the local equilibrium equations expressed as

$$\frac{\partial \sigma_{ji}}{\partial x_j} + b_i = \rho\,\ddot{u}_i \tag{7}$$

where b_i are body forces per unit volume, ρ is the mass density and $\ddot{u}_i$ the acceleration in the i-direction. Integrating directly we obtain three equilibrium equations for the force resultants as:

$$\begin{aligned} \frac{\partial N_{xx}}{\partial x} + \frac{\partial N_{yx}}{\partial y} + n_x &= \rho\,h\,\ddot{u} \\ \frac{\partial N_{xy}}{\partial x} + \frac{\partial N_{yy}}{\partial y} + n_y &= \rho\,h\,\ddot{v} \\ \frac{\partial Q_x}{\partial x} + \frac{\partial Q_y}{\partial y} + q &= \rho\,h\,\ddot{w}\ \ . \end{aligned} \tag{8}$$

Multiplying (7) by z and integrating through the thickness gives two additional equations:

$$\begin{aligned} \frac{\partial M_{xx}}{\partial x} + \frac{\partial M_{yx}}{\partial y} - Q_x + m_x &= \frac{1}{12}\,\rho\,h^3\,\ddot{\phi}_x \\ \frac{\partial M_{xy}}{\partial x} + \frac{\partial M_{yy}}{\partial y} - Q_y + m_y &= \frac{1}{12}\,\rho\,h^3\,\ddot{\phi}_y\ \ . \end{aligned} \tag{9}$$

In the above n_x, n_y, q are loads per unit area of plate and m_x, m_y are couples per unit area of plate.

In the theory, as presented here, the through thickness normal strain vanishes and the transverse normal stress does not appear. However, in introducing any constitutive equation we shall assume that the transverse normal stress is negligible and, thus, may be ignored. Here we shall consider a general anisotropic linear elastic material where the strain-stress relations are given in terms of the compliance as:

$$\boldsymbol{\epsilon} = \mathbf{C}\,\boldsymbol{\sigma} \tag{10}$$

with

$$\begin{aligned} \boldsymbol{\epsilon} &= \left[\begin{array}{ccccc} \epsilon_{xx} & \epsilon_{yy} & \gamma_{xy} & \gamma_{yz} & \gamma_{zx} \end{array} \right]^T \\ \boldsymbol{\sigma} &= \left[\begin{array}{ccccc} \sigma_{xx} & \sigma_{yy} & \tau_{xy} & \tau_{yz} & \tau_{zx} \end{array} \right]^T \end{aligned} \tag{11}$$

and the compliance array expressed by

$$\mathbf{C} = \left[\begin{array}{ccccc} C_{11} & C_{12} & C_{14} & C_{15} & C_{16} \\ C_{21} & C_{22} & C_{24} & C_{25} & C_{26} \\ C_{41} & C_{42} & C_{44} & C_{45} & C_{46} \\ C_{51} & C_{52} & C_{54} & C_{55} & C_{56} \\ C_{61} & C_{62} & C_{64} & C_{65} & C_{66} \end{array} \right] \quad . \tag{12}$$

In the above we have used Voigt notation to map tensor components to matrix form using the ordering

Matrix	1	2	4	5	6
Tensor	xx	yy	xy	yz	zx

.

Equation (10) may be inverted to yield the stress-strain relations given by

$$\boldsymbol{\sigma} = \mathbf{D}\,\boldsymbol{\epsilon} \tag{13}$$

these may then be introduced into the definitions for the force resultants given by (2) and (6) and combined with the strain displacement relations given in (3) and (4) to yield the plate constitutive relations

$$\left[\begin{array}{c} \mathbf{M} \\ \mathbf{N} \\ \mathbf{Q} \end{array} \right] = \left[\begin{array}{ccc} \mathbf{D}_{bb} & \mathbf{D}_{bm} & \mathbf{D}_{bs} \\ \mathbf{D}_{mb} & \mathbf{D}_{mm} & \mathbf{D}_{ms} \\ \mathbf{D}_{sb} & \mathbf{D}_{sm} & \mathbf{D}_{ss} \end{array} \right] \left[\begin{array}{c} \boldsymbol{\kappa}_b \\ \boldsymbol{\epsilon}_m \\ \boldsymbol{\gamma}_s \end{array} \right] \tag{14}$$

where

$$\mathbf{D}_{mm} = \int_h \begin{bmatrix} D_{11} & D_{12} & D_{14} \\ D_{21} & D_{22} & D_{24} \\ D_{41} & D_{42} & D_{44} \end{bmatrix} \mathrm{d}z \ , \quad \mathbf{D}_{mb} = \int_h \begin{bmatrix} D_{11} & D_{12} & D_{14} \\ D_{21} & D_{22} & D_{24} \\ D_{41} & D_{42} & D_{44} \end{bmatrix} z \, \mathrm{d}z$$

$$\mathbf{D}_{ms} = \int_h \begin{bmatrix} D_{15} & D_{16} \\ D_{25} & D_{26} \\ D_{45} & D_{46} \end{bmatrix} \mathrm{d}z \ , \qquad \mathbf{D}_{bb} = \int_h \begin{bmatrix} D_{11} & D_{12} & D_{14} \\ D_{21} & D_{22} & D_{24} \\ D_{41} & D_{42} & D_{44} \end{bmatrix} z^2 \, \mathrm{d}z$$

$$\mathbf{D}_{bs} = \int_h \begin{bmatrix} D_{15} & D_{16} \\ D_{25} & D_{26} \\ D_{45} & D_{46} \end{bmatrix} z \, \mathrm{d}z \ , \qquad \mathbf{D}_{ss} = \int_h \begin{bmatrix} D_{55} & D_{56} \\ D_{65} & D_{66} \end{bmatrix} \mathrm{d}z \ . \tag{15}$$

Some correction factors are necessary for quantities associated with the shear stresses and usual symmetry conditions hold so that

$$\mathbf{D}_{mb} = \mathbf{D}_{bm}^T \ ; \ \mathbf{D}_{ms} = \mathbf{D}_{sm}^T \ \text{ and } \ \mathbf{D}_{bs} = \mathbf{D}_{sb}^T \ . \tag{16}$$

Furthermore, for plates with homogeneous material properties, locating the reference surface at the middle of the plate results in

$$\int_h [\cdot] \, z \, \mathrm{d}z = 0 \tag{17}$$

so that (14) simplifies to

$$\begin{bmatrix} \mathbf{M} \\ \mathbf{N} \\ \mathbf{Q} \end{bmatrix} = \begin{bmatrix} \mathbf{D}_{bb} & \mathbf{0} & \mathbf{0} \\ \mathbf{0} & \mathbf{D}_{mm} & \mathbf{D}_{ms} \\ \mathbf{0} & \mathbf{D}_{sm} & \mathbf{D}_{ss} \end{bmatrix} \begin{bmatrix} \boldsymbol{\kappa}_b \\ \boldsymbol{\epsilon}_m \\ \boldsymbol{\gamma}_s \end{bmatrix} \tag{18}$$

and (15) is given by

$$\mathbf{D}_{mm} = \ h \begin{bmatrix} D_{11} & D_{12} & D_{14} \\ D_{21} & D_{22} & D_{24} \\ D_{41} & D_{42} & D_{44} \end{bmatrix} \ , \qquad \mathbf{D}_{ms} = k_c \, h \begin{bmatrix} D_{15} & D_{16} \\ D_{25} & D_{26} \\ D_{45} & D_{46} \end{bmatrix}$$

$$\mathbf{D}_{bb} = \frac{h^3}{12} \begin{bmatrix} D_{11} & D_{12} & D_{14} \\ D_{21} & D_{22} & D_{24} \\ D_{41} & D_{42} & D_{44} \end{bmatrix} \ , \qquad \mathbf{D}_{ss} = k_s \, h \begin{bmatrix} D_{55} & D_{56} \\ D_{65} & D_{66} \end{bmatrix} \tag{19}$$

where k_c and k_s are correction factors to account for non-uniform variation of the transverse shear stress components.

In (14) the membrane forces and strains are given by

$$\begin{aligned} \mathbf{N} &= \left[\begin{array}{ccc} N_{xx}\,, & N_{yy}\,, & N_{xy} \end{array} \right]^T \\ \boldsymbol{\epsilon}_m &= \left[\begin{array}{ccc} \dfrac{\partial u}{\partial x}\,, & \dfrac{\partial v}{\partial y}\,, & \left(\dfrac{\partial u}{\partial y} + \dfrac{\partial v}{\partial x}\right) \end{array} \right]^T \end{aligned} \tag{20}$$

the bending forces and curvature changes are given by

$$\begin{aligned} \mathbf{M} &= \left[\begin{array}{ccc} M_{xx}\,, & M_{yy}\,, & M_{xy} \end{array} \right]^T \\ \boldsymbol{\kappa}_b &= \left[\begin{array}{ccc} \dfrac{\partial \phi_x}{\partial x}\,, & \dfrac{\partial \phi_y}{\partial y}\,, & \left(\dfrac{\partial \phi_x}{\partial y} + \dfrac{\partial \phi_y}{\partial x}\right) \end{array} \right]^T \end{aligned} \tag{21}$$

and the transverse shear forces and strains are given by

$$\begin{aligned} \mathbf{Q} &= \left[\begin{array}{cc} Q_y\,, & Q_x \end{array} \right]^T \\ \boldsymbol{\gamma}_s &= \left[\begin{array}{cc} \left(\dfrac{\partial w}{\partial y} + \phi_y\right)\,, & \left(\dfrac{\partial w}{\partial x} + \phi_x\right) \end{array} \right]^T \quad . \end{aligned} \tag{22}$$

2.1 Variational Equations

Ignoring the inertial terms a standard variational form for the above equations may be written as

$$\delta\Pi = \int_A \left[\begin{array}{ccc} \delta\boldsymbol{\kappa}_b & \delta\boldsymbol{\epsilon}_m & \delta\boldsymbol{\gamma}_s \end{array} \right] \left[\begin{array}{ccc} \mathbf{D}_{bb} & \mathbf{D}_{bm} & \mathbf{D}_{bs} \\ \mathbf{D}_{mb} & \mathbf{D}_{mm} & \mathbf{D}_{ms} \\ \mathbf{D}_{sb} & \mathbf{D}_{sm} & \mathbf{D}_{ss} \end{array} \right] \left[\begin{array}{c} \boldsymbol{\kappa}_b \\ \boldsymbol{\epsilon}_m \\ \boldsymbol{\gamma}_s \end{array} \right] \mathrm{d}A - \delta\Pi_{ext} = 0 \tag{23}$$

where strain and virtual strains are expressed in terms of the displacement field given by (20), (21) and (22). The external variational term is given by

$$\begin{aligned} \delta\Pi_{ext} = &\int_A \left[\delta u\, n_x + \delta v\, n_y + \delta w\, q\right] \mathrm{d}A \\ &+ \int_A \left[\delta\phi_x\, m_x + \delta\phi_y\, m_y\right] \mathrm{d}A \quad . \end{aligned} \tag{24}$$

Alternatively, a three field form may be deduced and expressed as

$$\begin{aligned} \delta\Pi = &\int_A \delta\mathbf{E}\, \left[\mathbf{D}\,\mathbf{E} - \mathbf{S}\right] \mathrm{d}A + \int_A \delta\mathbf{S}\, \left[\mathbf{E}(\mathbf{U}) - \mathbf{E}\right] \mathrm{d}A \\ &+ \int_A \mathbf{E}(\delta\mathbf{U})\, \mathbf{S}\, \mathrm{d}A - \delta\Pi_{ext} = 0 \end{aligned} \tag{25}$$

where

$$\mathbf{S} = \left[\begin{array}{c} \mathbf{M} \\ \mathbf{N} \\ \mathbf{Q} \end{array} \right] \quad , \qquad \mathbf{E} = \left[\begin{array}{c} \boldsymbol{\kappa}_b \\ \boldsymbol{\epsilon}_m \\ \boldsymbol{\gamma}_s \end{array} \right] \quad , \qquad \mathbf{D} = \left[\begin{array}{ccc} \mathbf{D}_{bb} & \mathbf{D}_{bm} & \mathbf{D}_{bs} \\ \mathbf{D}_{mb} & \mathbf{D}_{mm} & \mathbf{D}_{ms} \\ \mathbf{D}_{sb} & \mathbf{D}_{sm} & \mathbf{D}_{ss} \end{array} \right] \tag{26}$$

and $\mathbf{U}$ denotes quantities expressed in terms of the displacement field.

For the case in which decoupling exists between the bending and the forces a Reissner type functional may be used. This is expressed here as

$$\begin{aligned} \delta\Pi = & \int_A \delta\boldsymbol{\kappa}_b \mathbf{D}_{bb}\, \boldsymbol{\kappa}_b \, \mathrm{d}A + \int_A \left[\begin{array}{cc} \delta\boldsymbol{\epsilon}_m & \delta\boldsymbol{\gamma}_s \end{array} \right] \left[\begin{array}{c} \mathbf{N} \\ \boldsymbol{Q} \end{array} \right] \mathrm{d}A - \delta\Pi_{ext} \\ & + \int_A \left[\begin{array}{cc} \delta\mathbf{N} & \delta\mathbf{Q} \end{array} \right] \left(\left[\begin{array}{c} \boldsymbol{\epsilon}_m \\ \boldsymbol{\gamma}_s \end{array} \right] - \left[\begin{array}{cc} \mathbf{C}_{mm} & \mathbf{C}_{ms} \\ \mathbf{C}_{sm} & \mathbf{C}_{ss} \end{array} \right] \left[\begin{array}{c} \mathbf{N} \\ \mathbf{Q} \end{array} \right] \right) \mathrm{d}A = 0 \end{aligned} \tag{27}$$

where

$$\left[\begin{array}{cc} \mathbf{C}_{mm} & \mathbf{C}_{ms} \\ \mathbf{C}_{sm} & \mathbf{C}_{ss} \end{array} \right] = \left[\begin{array}{cc} \mathbf{D}_{mm} & \mathbf{D}_{ms} \\ \mathbf{D}_{sm} & \mathbf{D}_{ss} \end{array} \right]^{-1} \tag{28}$$

is a compliance array for the plate forces.

3 Finite Element Interpolation

A linked interpolation between the transverse displacement, w, and rotation, $\boldsymbol{\phi}$ may be used to construct locking free plate bending elements. Here we consider the formulation for a 6-node triangular element with nodes positioned as shown in Fig. 2 and area coordinates ξ_i. The coordinates for points within the triangle are determined (sub-parametrically) using only the vertex nodes and the interpolation

$$\mathbf{x} = \left[\begin{array}{c} x \\ y \end{array} \right] = \sum_{i=1}^{3} \xi_i \, \tilde{\mathbf{x}}_i \quad . \tag{29}$$

Thus, here the mid-side nodes are always assumed to lie at the mid-point of a straight sided triangle.

To construct the shape functions for the displacement field within each triangle we begin by defining the usual quadratic shape functions at the nodes

$$\begin{aligned} N_i \quad &= \xi_i \, (2\,\xi_i - 1) \quad ; \quad i = 1, 2, 3 \\ N_{i+3} &= 4\,\xi_i \, \xi_j \quad \text{where} \quad j = mod(i, 3) + 1 \quad . \end{aligned} \tag{30}$$

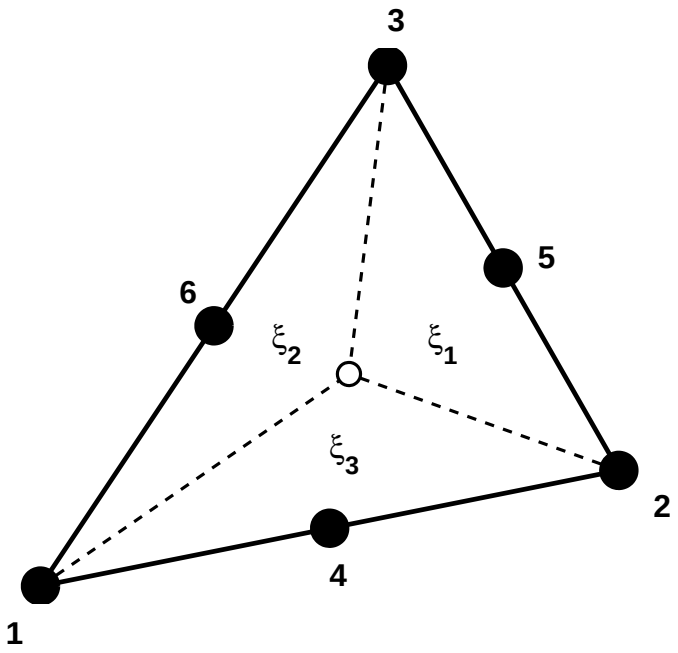

Figure 2: 6-node triangular element and area coordinates

These are used directly to interpolate the in-plane displacement field over the triangle as

$$\mathbf{u} = \left[\begin{array}{c} u \\ v \end{array} \right] = \sum_{i=1}^{6} N_i \, \tilde{\mathbf{u}}_i \tag{31}$$

and the rotation field as

$$\boldsymbol{\phi} = \left[\begin{array}{c} \phi_x \\ \phi_y \end{array} \right] = \sum_{i=1}^{6} N_i \, \tilde{\boldsymbol{\phi}}_i \quad . \tag{32}$$

The transverse displacement is interpolated as

$$w = \sum_{i=1}^{6} N_i \, \tilde{w}_i + \sum_{i=1}^{3} P_i \, \alpha_{i+3} + N_b \, \tilde{w}_b \tag{33}$$

where

$$P_i = \xi_i \, \xi_j (\xi_j - \xi_i) \quad \text{with} \quad j = \mod (i,3) + 1 \tag{34}$$

are cubic terms within the triangle, the α_m are associated with the side containing the mid-side m-node [see Fig. (3)] and N_b is the interior cubic bubble mode

$$N_b = \xi_1 \, \xi_2 \, \xi_3 \tag{35}$$

which is added to complete the cubic field.

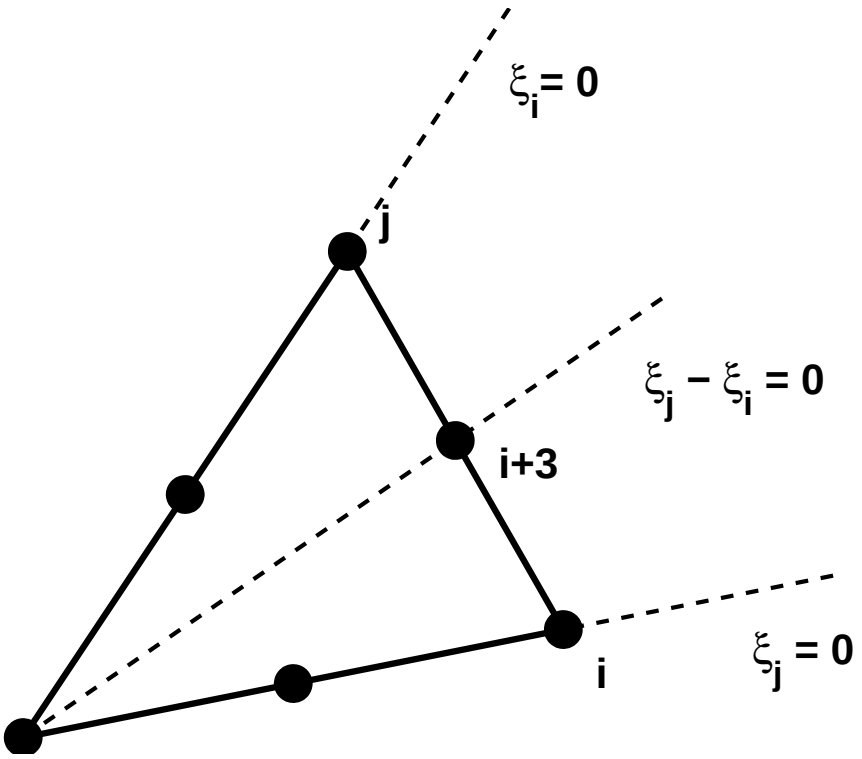

Figure 3: Zero lines for P_i

The goal now is to define the α_m in terms of the rotation parameters associated with the side containing the m-node. This leads to the notion of a *linked* interpolation in which the w displacement is given in terms of nodal values of both w and $\boldsymbol{\phi}$. The element will remain conforming provided such construction involves parameters which are associated only with the side containing the m-node.

To construct the linked interpolation we consider a typical side defined by nodes $i - m - j$ as shown in Fig. 4. Along this side we consider the

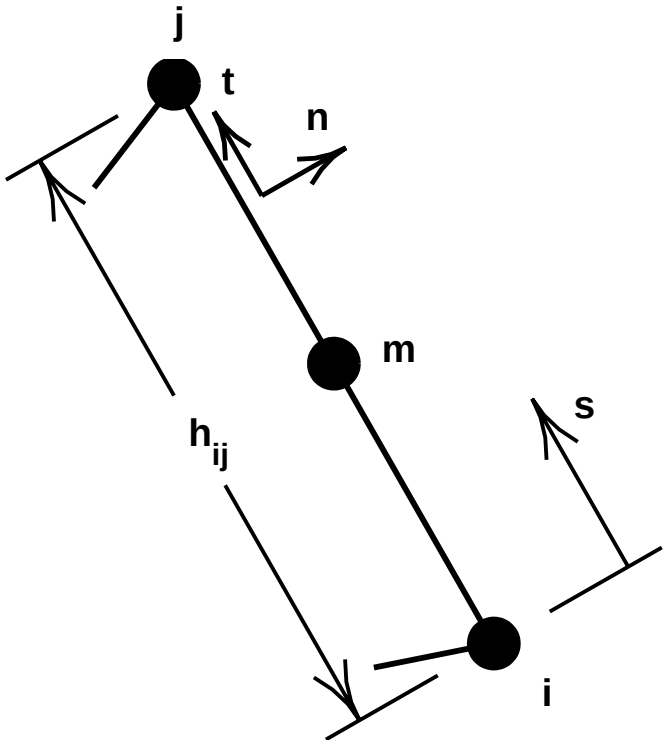

Figure 4: Side of 6-node triangle for linked derivation

tangential component of the transverse shearing strain given by

$$\gamma_s = \frac{\partial w}{\partial s} + \phi_s \tag{36}$$

where s is the tangential coordinate and n is the normal direction to the side. For this side and an origin for s defined at the i-node, the values of the area coordinates satisfy

$$\xi_k = 0 \quad \text{and} \quad \xi_i + \xi_j = 1 \quad . \tag{37}$$

Using Eq. (37) we can write the shape functions entirely in terms of ξ_j as

$$\begin{aligned} N_i &= 1 - 3\,\xi_j + 2\,\xi_j^2 \\ N_j &= \xi_j(2\,\xi_j - 1) \\ N_m &= 4\,(\xi_j - \xi_j^2) \quad \text{where} \quad m = i + 3 \\ P_i &= -\,\xi_j + 3\,\xi_j^2 - 2\,\xi_j^3 \quad . \end{aligned} \tag{38}$$

The derivative of w in the s direction may now be expressed as

$$\frac{\partial w}{\partial s} = \frac{\partial w}{\partial \xi_j}\,\frac{\partial \xi_j}{\partial s} \tag{39}$$

where

$$s = \xi_j\, h_{ij} \quad \text{giving} \quad \frac{\partial \xi_j}{\partial s} = \frac{1}{h_{ij}} \tag{40}$$

in which h_{ij} is the length of the ij-side

$$h_{ij} = \left[(\tilde{x}_j - \tilde{x}_i)^2 + (\tilde{y}_j - \tilde{y}_i)^2\right]^{1/2} \quad . \tag{41}$$

The tangential rotation displacement, ϕ_s, along the ij side may be expressed as

$$\phi_s = \mathbf{t}_{ij}^T \left[N_i\, \tilde{\boldsymbol{\phi}}_i + N_j\, \tilde{\boldsymbol{\phi}}_j + N_m\, \tilde{\boldsymbol{\phi}}_m\right] \tag{42}$$

where $\mathbf{t}_{ij}$ is the unit tangent vector along the boundary as shown in Fig. 4 and may be expressed as

$$\mathbf{s}_{ij} = \cos\varphi_{ij}\, \mathbf{e}_x + \sin\varphi_{ij}\, \mathbf{e}_y \tag{43}$$

where

$$\cos\varphi_{ij} = (\tilde{x}_j - \tilde{x}_i)/h_{ij} \quad \text{and} \quad \sin\varphi_{ij} = (\tilde{y}_j - \tilde{y}_i)/h_{ij}$$

and $\mathbf{e}_x$, $\mathbf{e}_y$ are the unit vectors along the x and y-directions, respectively.

The goal of the linked derivation is to now express the α_m in terms of the nodal rotation parameters along the ij side so that all quadratic terms in ξ_j in the tangential shear strain are eliminated. Carrying out this step for the above interpolations yields

$$\alpha_m = \frac{h_{ij}}{3}\, \mathbf{t}_{ij}^T \left[\tilde{\boldsymbol{\phi}}_i + \tilde{\boldsymbol{\phi}}_j - 2\, \tilde{\boldsymbol{\phi}}_m\right] \quad . \tag{44}$$

Returning to the definition of the shape functions over the entire triangle we now may write the transverse displacement interpolation as

$$\begin{aligned} w &= \sum_{i=1}^{3} \xi_i(2\,\xi_i - 1)\, \tilde{w}_i + \sum_{i=1}^{3} 4\xi_i\xi_j\, \tilde{w}_{i+3} + \xi_1\xi_2\xi_3\, \tilde{w}_b \\ &\quad + \sum_{i=1}^{3} \frac{h_{ij}}{3}\xi_i\xi_j(\xi_j - \xi_i)\mathbf{t}_{ij}^T \left[\tilde{\boldsymbol{\phi}}_i + \tilde{\boldsymbol{\phi}}_j - 2\, \tilde{\boldsymbol{\phi}}_{i+3}\right] \\ &= \sum_{i=1}^{6} N_i\, \tilde{w}_i + \sum_{i=1}^{6} N_i^{w\phi} \mathbf{t}^T \tilde{\boldsymbol{\phi}}_i + N_b\, \tilde{w}_b \quad . \end{aligned} \tag{45}$$

The interpolation for the rotation is given by Eq. (32).

In deriving the expressions for the strains from the above interpolations an enhanced term is added to the bending values. The enhanced term is deduced from bubble modes which for the rotation field are given by

$$\begin{aligned} \boldsymbol{\phi}^{en} &= \sum_{i=1}^{3} (\xi_i - \frac{1}{3})\, N_b\, \tilde{\boldsymbol{\beta}}_i + (\boldsymbol{\nabla} N_b) N_b\, \tilde{\phi}_b \\ &= \sum_{i=1}^{3} N_i^{\beta}\, \tilde{\boldsymbol{\beta}}_i + \mathbf{N}_b^{\phi}\, \tilde{\phi}_b \quad . \end{aligned} \tag{46}$$

Finally, membrane and transverse shear forces are assumed as linear quantities within each element and expressed by the interpolation

$$\begin{aligned} \mathbf{N} &= \sum_{i=1}^{3} \xi_i\, \tilde{\mathbf{N}}_i \\ \mathbf{Q} &= \sum_{i=1}^{3} \xi_i\, \tilde{\mathbf{Q}}_i + \boldsymbol{\nabla} N_b\, \tilde{Q}_b \end{aligned} \tag{47}$$

where in addition to the linear terms in $\mathbf{Q}$ a gradient of the bubble is included to ensure that the space for shears is a subspace of that for the transverse displacements [7, 8, 9].

3.1 Matrix formulation

The above formulation may be put into a matrix form by introducing strain-displacement arrays for each of the parts. Accordingly, we have

$$\boldsymbol{\epsilon}_m = \sum_{i=1}^{6} \mathbf{B}_i\, \tilde{\mathbf{u}}_i \tag{48}$$

where

$$\mathbf{B}_i = \begin{bmatrix} N_{i,x} & 0 \\ 0 & N_{i,y} \\ N_{i,y} & N_{i,x} \end{bmatrix} \tag{49}$$

in which $N_{i,x} = \partial N_i / \partial x$, etc. are derivatives of shape functions.

The bending strains are given by

$$\boldsymbol{\kappa}_b = \sum_{i=1}^{6} \mathbf{B}_i^b \, \tilde{\mathbf{w}}_i + \sum_{i=1}^{3} \mathbf{B}_i^{b\beta} \, \tilde{\boldsymbol{\beta}}_i + \mathbf{B}^{b\phi} \, \tilde{\phi}_b \tag{50}$$

where $\tilde{\mathbf{w}}_i = [w_i \, , \, (\tilde{\phi}_x)_i \, , \, (\tilde{\phi}_y)_i]^T$ and

$$\begin{aligned} \mathbf{B}_i^b &= \begin{bmatrix} 0 & N_{i,x} & 0 \\ 0 & 0 & N_{i,y} \\ 0 & N_{i,y} & N_{i,x} \end{bmatrix} \\ \mathbf{B}_i^{b\beta} &= \begin{bmatrix} N_{i,x}^\beta & 0 \\ 0 & N_{i,y}^\beta \\ N_{i,y}^\beta & N_{i,x}^\beta \end{bmatrix} \quad \text{and} \\ \mathbf{B}^{b\phi} &= \begin{bmatrix} N_{b,x} \, N_{b,x} + N_{b,xx} \, N_b \\ N_{b,y} \, N_{b,y} + N_{b,yy} \, N_b \\ 2 \, (N_{b,x} \, N_{b,y} + N_{b,xy} \, N_b) \end{bmatrix} \quad . \quad . \end{aligned} \tag{51}$$

Finally, the transverse shearing strains may be expressed as

$$\boldsymbol{\gamma}_s = \sum_{i=1}^{6} \mathbf{B}_i^s \, \tilde{\mathbf{w}}_i + \mathbf{B}^{sw} \, \tilde{w}_b + \sum_{i=1}^{3} \mathbf{B}_i^{s\beta} \, \tilde{\boldsymbol{\beta}}_i + \mathbf{B}^{s\phi} \, \tilde{\phi}_b \tag{52}$$

where

$$\begin{aligned} \mathbf{B}_i^s &= \begin{bmatrix} N_{i,y} & N_{i,y}^{w\phi} \, t_x & N_i + N_{i,y}^{w\phi} \, t_y \\ N_{i,x} & N_i + N_{i,x}^{w\phi} \, t_x & N_{i,x}^{w\phi} \, t_y \end{bmatrix} \\ \mathbf{B}^{sw} &= \begin{bmatrix} N_{b,y} \\ N_{b,x} \end{bmatrix} \\ \mathbf{B}_i^{s\beta} &= \begin{bmatrix} 0 & N_i^\beta \\ N_i^\beta & 0 \end{bmatrix} \quad \text{and} \\ \mathbf{B}^{s\phi} &= \begin{bmatrix} N_{b,y} \, N_b \\ N_{b,x} \, N_b \end{bmatrix} \quad . \end{aligned} \tag{53}$$

The above may be collected together as

$$\begin{bmatrix} \boldsymbol{\kappa}_b \\ \boldsymbol{\epsilon}_m \\ \boldsymbol{\gamma}_s \end{bmatrix} = \begin{bmatrix} \mathbf{0} & \mathbf{B}_i^b & \mathbf{B}_j^{b\beta} & \mathbf{B}^{b\phi} & \mathbf{0} \\ \mathbf{B}_i & \mathbf{0} & \mathbf{0} & \mathbf{0} & \mathbf{0} \\ \mathbf{0} & \mathbf{B}_i^s & \mathbf{B}_j^{s\beta} & \mathbf{B}^{s\phi} & \mathbf{B}^{sw} \end{bmatrix} \begin{bmatrix} \tilde{\mathbf{u}}_i \\ \tilde{\mathbf{w}}_i \\ \tilde{\boldsymbol{\beta}}_j \\ \tilde{\phi}_b \\ \tilde{w}_b \end{bmatrix} \qquad \begin{matrix} i = 1, 2, \ldots, 6 \\ j = 1, 2, 3 \end{matrix} \tag{54}$$

in which summations are assumed over the range of the indices.

3.2 Element arrays

We are now able to construct the arrays appearing in Eq. (27). Accordingly, inserting (54) we obtain for the bending term

$$\int_A \delta\boldsymbol{\kappa}_b\, \mathbf{D}_{bb}\, \boldsymbol{\kappa}_b \,\mathrm{d}A = \begin{bmatrix} \delta\tilde{\mathbf{w}}_i & \delta\tilde{\boldsymbol{\beta}}_j & \delta\tilde{\phi}_b \end{bmatrix} \begin{bmatrix} \mathbf{A}_{ik}^{ww} & \mathbf{A}_{il}^{w\beta} & \mathbf{A}_{i}^{w\phi} \\ \mathbf{A}_{jk}^{\beta w} & \mathbf{A}_{jl}^{\beta\beta} & \mathbf{A}_{j}^{\beta\phi} \\ \mathbf{A}_{k}^{\phi w} & \mathbf{A}_{l}^{\phi\beta} & A^{\phi\phi} \end{bmatrix} \begin{bmatrix} \tilde{\mathbf{w}}_k \\ \tilde{\boldsymbol{\beta}}_l \\ \tilde{\phi}_b \end{bmatrix} \qquad \begin{matrix} i,k = 1,2,\ldots,6 \\ j,l = 1,2,3 \end{matrix} \tag{55}$$

where

$$\begin{aligned} \mathbf{A}_{ik}^{ww} &= \int_A (\mathbf{B}_i^b)^T\, \mathbf{D}_{bb}\, \mathbf{B}_k^b \,\mathrm{d}A & \mathbf{A}_{il}^{w\beta} &= \int_A (\mathbf{B}_i^b)^T\, \mathbf{D}_{bb}\, \mathbf{B}_l^{b\beta} \,\mathrm{d}A \\ \mathbf{A}_{i}^{w\phi} &= \int_A (\mathbf{B}_i^b)^T\, \mathbf{D}_{bb}\, \mathbf{B}^{b\phi} \,\mathrm{d}A & \mathbf{A}_{jk}^{\beta w} &= \int_A (\mathbf{B}_j^{b\beta})^T\, \mathbf{D}_{bb}\, \mathbf{B}_k^b \,\mathrm{d}A \\ \mathbf{A}_{jl}^{\beta\beta} &= \int_A (\mathbf{B}_j^{b\beta})^T\, \mathbf{D}_{bb}\, \mathbf{B}_l^{b\beta} \,\mathrm{d}A & \mathbf{A}_{j}^{\beta\phi} &= \int_A (\mathbf{B}_j^{b\beta})^T\, \mathbf{D}_{bb}\, \mathbf{B}^{b\phi} \,\mathrm{d}A \\ \mathbf{A}_{k}^{\phi w} &= \int_A (\mathbf{B}^{b\phi})^T\, \mathbf{D}_{bb}\, \mathbf{B}_k^b \,\mathrm{d}A & \mathbf{A}_{l}^{\phi\beta} &= \int_A (\mathbf{B}^{b\phi})^T\, \mathbf{D}_{bb}\, \mathbf{B}_l^{b\beta} \,\mathrm{d}A \\ A^{\phi\phi} &= \int_A (\mathbf{B}^{b\phi})^T\, \mathbf{D}_{bb}\, \mathbf{B}^{b\phi} \,\mathrm{d}A \quad . \end{aligned} \tag{56}$$

The compliance term in (27) is expressed by

$$\begin{aligned} -\int_A \begin{bmatrix} \delta\mathbf{N} & \delta\mathbf{Q} \end{bmatrix} \begin{bmatrix} \mathbf{C}_{mm} & \mathbf{C}_{ms} \\ \mathbf{C}_{sm} & \mathbf{C}_{ss} \end{bmatrix} \begin{bmatrix} \mathbf{N} \\ \mathbf{Q} \end{bmatrix} \mathrm{d}A = \\ \begin{bmatrix} \delta\tilde{\mathbf{N}}_j & \delta\tilde{\mathbf{Q}}_j & \delta\tilde{Q}_b \end{bmatrix} \begin{bmatrix} \mathbf{H}_{jl}^{mm} & \mathbf{H}_{jl}^{ms} & \mathbf{H}_{j}^{mq} \\ \mathbf{H}_{jl}^{sm} & \mathbf{H}_{jl}^{ss} & \mathbf{H}_{j}^{sq} \\ \mathbf{H}_{l}^{qm} & \mathbf{H}_{l}^{qs} & H^{qq} \end{bmatrix} \begin{bmatrix} \tilde{\mathbf{N}}_l \\ \tilde{\mathbf{Q}}_l \\ \tilde{Q}_b \end{bmatrix} \end{aligned} \tag{57}$$

where

$$
\begin{aligned}
\mathbf{H}^{mm}_{jl} &= -\int_A \xi_j\, \mathbf{C}_{mm}\, \xi_l \,\mathrm{d}A & \mathbf{H}^{ms}_{jl} &= -\int_A \xi_j\, \mathbf{C}_{ms}\, \xi_l \,\mathrm{d}A \\
\mathbf{H}^{mq}_{j} &= -\int_A \xi_j\, \mathbf{C}_{ms}\, \boldsymbol{\nabla} N_b \,\mathrm{d}A & \mathbf{H}^{sm}_{jl} &= -\int_A \xi_j\, \mathbf{C}_{sm}\, \xi_l \,\mathrm{d}A \\
\mathbf{H}^{ss}_{jl} &= -\int_A \xi_j\, \mathbf{C}_{ss}\, \xi_l \,\mathrm{d}A & \mathbf{H}^{sq}_{j} &= -\int_A \xi_j\, \mathbf{C}_{ss}\, \boldsymbol{\nabla} N_b \,\mathrm{d}A \\
\mathbf{H}^{qm}_{l} &= -\int_A (\boldsymbol{\nabla} N_b)^T\, \mathbf{C}_{sm}\, \xi_l \,\mathrm{d}A & \mathbf{H}^{qs}_{l} &= -\int_A (\boldsymbol{\nabla} N_b)^T\, \mathbf{C}_{ss}\, \xi_l \,\mathrm{d}A \\
H^{qq} &= -\int_A (\boldsymbol{\nabla} N_b)^T\, \mathbf{C}_{ss}\, \boldsymbol{\nabla} N_b \,\mathrm{d}A \quad .
\end{aligned}
\tag{58}
$$

The coupling term between the forces and strains is given by

$$
\int_A \begin{bmatrix} \delta\mathbf{N} & \delta\mathbf{Q} \end{bmatrix} \begin{bmatrix} \boldsymbol{\epsilon}_m \\ \boldsymbol{\gamma}_s \end{bmatrix} \mathrm{d}A =
$$

$$
\begin{bmatrix} \delta\tilde{\mathbf{N}}_j & \delta\tilde{\mathbf{Q}}_j & \delta\tilde{Q}_b \end{bmatrix} \begin{bmatrix} \mathbf{G}^{mu}_{jk} & \mathbf{0} & \mathbf{0} & \mathbf{0} & \mathbf{0} \\ \mathbf{0} & \mathbf{G}^{sw}_{jk} & \mathbf{G}^{s\beta}_{jl} & \mathbf{G}^{s\phi}_{j} & \mathbf{G}^{sb}_{j} \\ \mathbf{0} & \mathbf{G}^{qw}_{k} & \mathbf{G}^{q\beta}_{l} & G^{q\phi} & G^{qb} \end{bmatrix} \begin{bmatrix} \tilde{\mathbf{u}}_k \\ \tilde{\mathbf{w}}_k \\ \tilde{\boldsymbol{\beta}}_l \\ \tilde{\phi}_b \\ \tilde{w}_b \end{bmatrix}
\tag{59}
$$

$$
\begin{aligned}
\mathbf{G}^{mu}_{jk} &= \int_A \xi_j\, \mathbf{B}_k \,\mathrm{d}A \\
\mathbf{G}^{sw}_{jk} &= \int_A \xi_j\, \mathbf{B}^s_k \,\mathrm{d}A & \mathbf{G}^{s\beta}_{jl} &= \int_A \xi_j\, \mathbf{B}^{s\beta}_l \,\mathrm{d}A \\
\mathbf{G}^{s\phi}_{j} &= \int_A \xi_j\, \mathbf{B}^{s\phi} \,\mathrm{d}A & \mathbf{G}^{sb}_{j} &= \int_A \xi_j\, \mathbf{B}^{sw} \,\mathrm{d}A \\
\mathbf{G}^{qw}_{k} &= \int_A (\boldsymbol{\nabla} N_b)^T\, \mathbf{B}^s_k \,\mathrm{d}A & \mathbf{G}^{q\beta}_{l} &= \int_A (\boldsymbol{\nabla} N_b)^T\, \mathbf{B}^{s\beta}_l \,\mathrm{d}A \\
G^{q\phi} &= \int_A (\boldsymbol{\nabla} N_b)^T\, \mathbf{B}^{s\phi} \,\mathrm{d}A & G^{qb} &= \int_A (\boldsymbol{\nabla} N_b)^T\, \mathbf{B}^{sw} \,\mathrm{d}A \quad .
\end{aligned}
\tag{60}
$$

The above arrays are assembled into a total element array as

$$
\mathbf{K}\,\tilde{\mathbf{U}} = \mathbf{F} \tag{61}
$$

where the unknowns are ordered as

$$\tilde{\mathbf{U}} = \left[\begin{array}{cccccccc} \tilde{\mathbf{u}}_k & \tilde{\mathbf{w}}_k & \tilde{\boldsymbol{\beta}}_l & \tilde{\phi}_b & \tilde{w}_b & \tilde{\mathbf{N}}_l & \tilde{\mathbf{Q}}_l & \tilde{Q}_b \end{array} \right]^T \; ; \quad \begin{array}{l} k = 1, 2, \ldots, 6 \\ l = 1, 2, 3 \end{array} \tag{62}$$

the assembled *stiffness* array is given by

$$\mathbf{K} = \left[\begin{array}{cccccccc} \mathbf{0} & \mathbf{0} & \mathbf{0} & \mathbf{0} & \mathbf{0} & \mathbf{G}_{il}^{um} & \mathbf{0} & \mathbf{0} \\ \mathbf{0} & \mathbf{A}_{ik}^{ww} & \mathbf{A}_{il}^{w\beta} & \mathbf{A}_{i}^{w\phi} & \mathbf{0} & \mathbf{0} & \mathbf{G}_{il}^{ws} & \mathbf{G}_{i}^{wq} \\ \mathbf{0} & \mathbf{A}_{jk}^{\beta w} & \mathbf{A}_{jl}^{\beta\beta} & \mathbf{A}_{j}^{\beta\phi} & \mathbf{0} & \mathbf{0} & \mathbf{G}_{jl}^{\beta s} & \mathbf{G}_{j}^{\beta q} \\ \mathbf{0} & \mathbf{A}_{k}^{\phi w} & \mathbf{A}_{l}^{\phi\beta} & A^{\phi\phi} & \mathbf{0} & \mathbf{0} & \mathbf{G}_{l}^{\phi s} & G^{\phi q} \\ \mathbf{0} & \mathbf{0} & \mathbf{0} & \mathbf{0} & 0 & \mathbf{0} & \mathbf{G}_{l}^{bs} & G^{bq} \\ \mathbf{G}_{jk}^{mu} & \mathbf{0} & \mathbf{0} & \mathbf{0} & \mathbf{0} & \mathbf{H}_{jl}^{mm} & \mathbf{H}_{jl}^{ms} & \mathbf{H}_{j}^{mq} \\ \mathbf{0} & \mathbf{G}_{jk}^{sw} & \mathbf{G}_{jl}^{s\beta} & \mathbf{G}_{j}^{s\phi} & \mathbf{G}_{j}^{sb} & \mathbf{H}_{jl}^{sm} & \mathbf{H}_{jl}^{ss} & \mathbf{H}_{j}^{sq} \\ \mathbf{0} & \mathbf{G}_{k}^{qw} & \mathbf{G}_{l}^{q\beta} & G^{q\phi} & G^{qb} & \mathbf{H}_{l}^{qm} & \mathbf{H}_{l}^{qs} & H^{qq} \end{array} \right] \tag{63}$$

and $\mathbf{F}$ is the assembled load vector. The load vector is computed from (24) and is given by

$$\mathbf{F} = \left[\begin{array}{cccccccc} \mathbf{F}_i^u & \mathbf{F}_i^w & \mathbf{F}_j^\beta & F_b^\phi & F_b^w & \mathbf{F}_j^N & \mathbf{F}_j^Q & F_q \end{array} \right]^T \; ; \quad \begin{array}{l} i = 1, 2, \ldots, 6 \\ j = 1, 2, 3 \end{array} \tag{64}$$

where

$$\begin{aligned} \mathbf{F}_i^u &= \int_A N_i \left[\begin{array}{c} n_x \\ n_y \end{array} \right] \mathrm{d}A \qquad & \mathbf{F}_i^w &= \int_A \left[\begin{array}{l} N_i\, q \\ N_i\, m_x + N_i^{w\phi}\, q\, t_x \\ N_i\, m_y + N_i^{w\phi}\, q\, t_y \end{array} \right] \mathrm{d}A \\ \mathbf{F}_j^\beta &= \int_A N_j^\beta \left[\begin{array}{c} m_x \\ m_y \end{array} \right] \mathrm{d}A \qquad & F_b^\phi &= \int_A \left(N_{b,x}\, m_x + N_{b,y}\, m_y \right)\, N_b \, \mathrm{d}A \\ F_b^w &= \int_A N_b\, q \, \mathrm{d}A & \mathbf{F}_j^N &= \mathbf{0} \\ \mathbf{F}_j^Q &= \mathbf{0} & F_q &= 0 \quad . \end{aligned} \tag{65}$$

In Appendix A we present additional details on the programming for the above development.

4 Examples

4.1 Reissner-Mindlin plate solutions

An accurate "exact" solution to problems modeled by the Reissner-Mindlin theory presents considerable difficulty. One approach is to split the displace-

ment as

$$w = w_b + w_s \quad \text{with} \quad \phi_x = -\frac{\partial w}{\partial x} \quad ; \quad \phi_y = -\frac{\partial w}{\partial y} \tag{66}$$

in which w_b denotes a *bending* solution and w_s a *shear* solution component. Inserting the above into the strain expressions gives

$$\boldsymbol{\gamma}_s = \left\{ \begin{array}{c} \dfrac{\partial w_s}{\partial y} \\ \dfrac{\partial w_s}{\partial x} \end{array} \right\} \tag{67}$$

and

$$\boldsymbol{\chi}_b = - \left\{ \begin{array}{c} \dfrac{\partial^2 w_b}{\partial x^2} \\ \dfrac{\partial^2 w_b}{\partial y^2} \\ 2\,\dfrac{\partial^2 w_b}{\partial x \partial y} \end{array} \right\} . \tag{68}$$

Using this split we may construct the equilibrium equations for an isotropic case as:

$$D\,\nabla^4 w_b = q \tag{69}$$

and

$$\kappa\,G\,h\,\nabla^2 w_s = -\,q \quad . \tag{70}$$

In the above ∇^4 is the bi-harmonic operator and ∇^2 the Laplacian operator. These equations create valid solutions only for situations in which the shear forces from the bending solution are identical to those of the shear solution. This leads to the requirement

$$\kappa\,G\,h\,w_s = -\,D\,\nabla^2 w_b + C \tag{71}$$

and here there are few cases which exist. One possibility to construct a solution is to use

$$\nabla^4 w = \nabla^4 w_b + \nabla^4 w_s = \frac{q}{D} - \frac{\nabla^2 q}{\kappa\,G\,h} = \frac{1}{D}\left[q - \frac{t^2\,\nabla^2 q}{6\,\kappa\,(1-\nu)} \right] \tag{72}$$

by selecting a w whereby the generating q can be easily determined via (72).

4.2 Error norm

To facilitate the comparison of convergence properties for the element we use an energy norm measure. The energy is computed by integrating the work under transverse loading. Accordingly, we compute only the work term

$$E_h = \int_A w\, q \, \mathrm{d}A \quad . \tag{73}$$

where E_h is the approximation from a mesh with element size h. This results in a quantity which is twice the equivalent of the stored energy; note that since a mixed principle is used, the computation of the actual stored energy is much more difficult to obtain than the simple expression given by (73). Furthermore, we note that use of a mixed principle implies that no bounding of energy can be expected. Convergence in the above energy may occur from either above or below – or even non-monotonically. Thus, for the comparison of energy error we use the expression

$$\|e\| = \|E_h - E\| \tag{74}$$

where $\|\cdot\|$ is the discrete L^2 norm and E is the *exact* energy for the problem.[1]

4.3 Numerical results

The classical problem for several rectangular plates subjected to lateral loading is used to demonstrate the performance of the linked triangular element. Three types of boundary conditions are considered:

1. SS1: Soft simply supported conditions with

   $$w = 0 \;\; ; \;\; M_{nn} = 0 \;\; \text{and} \;\; M_{ns} = 0$$

   on all boundaries; n is the outer normal direction and s a tangent direction on the boundary.

2. SS2: Hard simply supported conditions with

   $$w = 0 \;\; ; \;\; \phi_s = 0 \;\; \text{and} \;\; M_{ns} = 0\,.$$

3. CL: Clamped conditions with

   $$w = 0 \;\; ; \;\; \phi_n = 0 \;\; \text{and} \;\; \phi_s = 0\,.$$

[1] The value for the work can be replaced by a very accurate solution when no exact solution is available.

4.3.1 Simply supported (SS2) plate

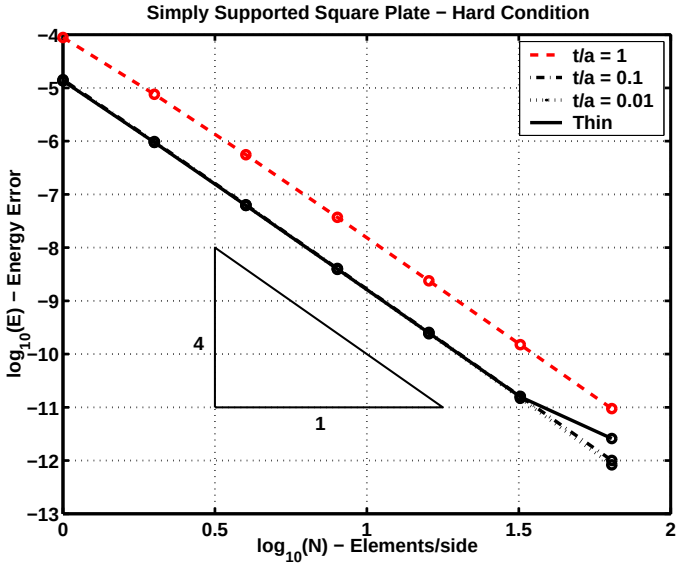

Figure 5: Energy error for square, sinusoidal loaded, simply supported plate - Hard (SS2) boundary conditions

As a first example we consider the solution of a rectangular plate subjected to the loading

$$q = q_0 \sin\frac{\pi\, x}{a} \sin\frac{\pi\, y}{b}$$

where a and b are the side lengths in the x and y directions, respectively; and q_0 is a loading intensity. An exact solution may be computed from (66) to (72) in which the two displacements are expressed as

$$w_b = \tilde{w}_b \sin\frac{\pi\, x}{a} \sin\frac{\pi\, y}{b}$$
$$w_s = \tilde{w}_s \sin\frac{\pi\, x}{a} \sin\frac{\pi\, y}{b}$$

The values for $\tilde{w}_b$ and $\tilde{w}_s$ may be determined from (69) and (70), respectively. One can verify that (71) is satisfied with $C = 0$.

The convergence properties for the energy error are shown in Fig. 5.

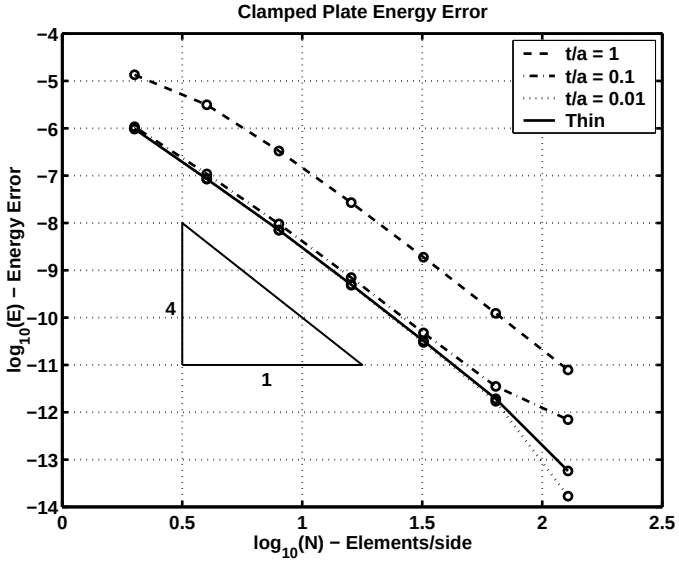

Figure 6: Energy error for square, clamped plate - With shear deformation

4.3.2 Clamped plate

For a clamped plate a solution based on Eqs (66) to (72) has been given by Chinosi and Lovadina [10]. Using an inverse method we may write the solution as:

$$w_b = \frac{1}{3}\, x^3(x-1)^3 y^3(y-1)^3$$

$$w_s = -\frac{t^2}{6\kappa(1-\nu)}\, \nabla^2 w_b$$

which gives the load

$$\begin{aligned} q = D\ \big[& 12y(y-1)(5x(x-1)+1)(2y^2(y-1)^2 + x(x-1)(5y(y-1)+1) \\ + \ & 12x(x-1)(5y(y-1)+1)(2x^2(x-1)^2 + y(y-1)(5x(x-1)+1)\big]\ . \end{aligned}$$

This solution is used to illustrate the convergence of the energy error for a clamped plate as shown in Fig. 6.

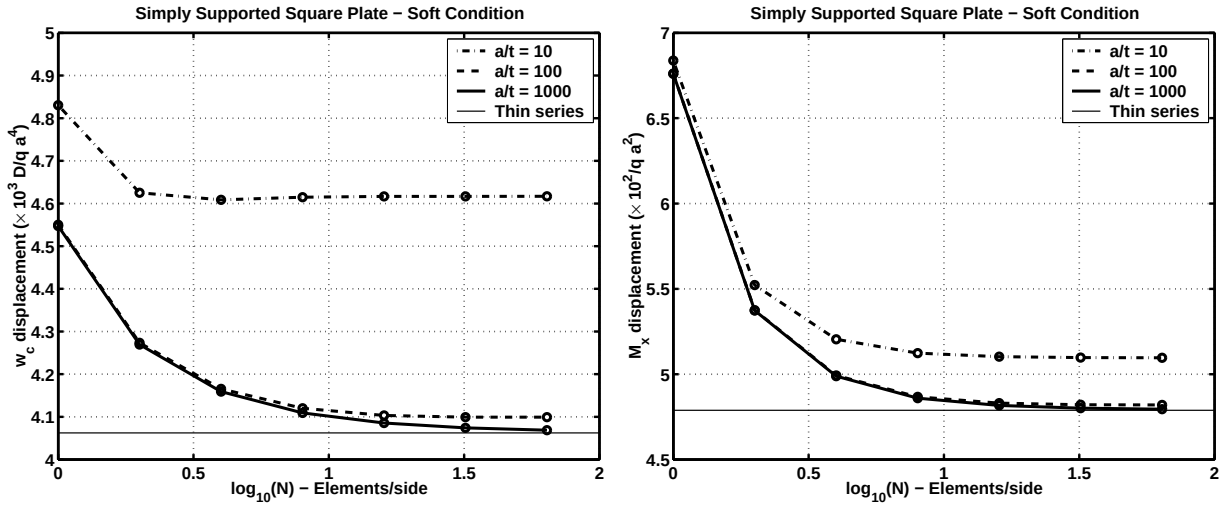

Figure 7: Center displacement and moment for square, uniformly loaded plate with soft (SS1) simply supported boundary conditions

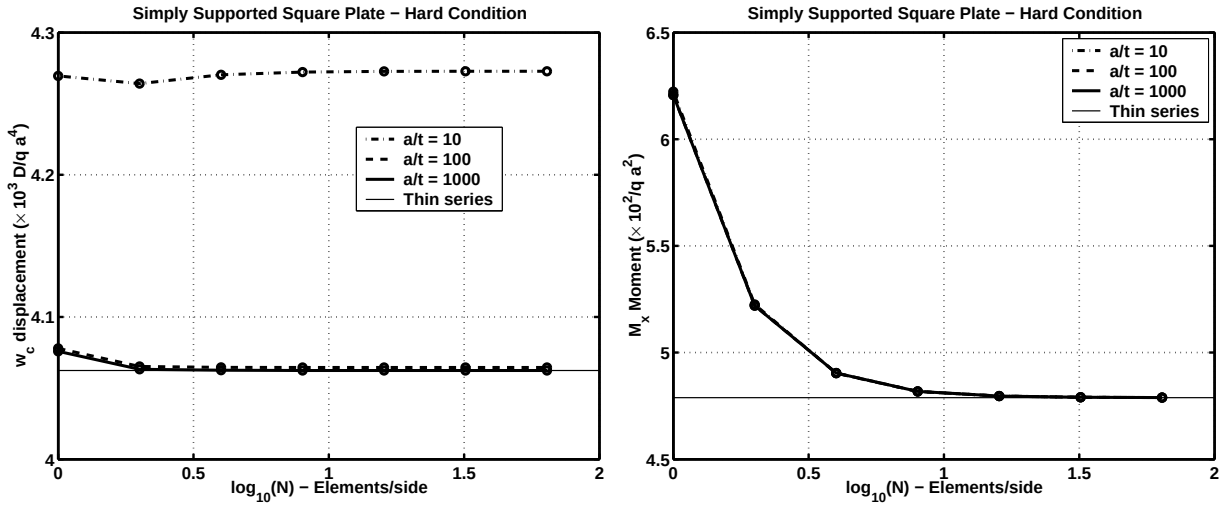

Figure 8: Center displacement and moment for square, uniformly loaded plate with hard (SS2) simply supported boundary conditions

4.3.3 Uniformly loaded, simply supported plates

The behavior of simply supported plates with hard and soft type boundary conditions is illustrated for a uniformly loaded condition. The convergence of center displacements and moment are shown in Figs 7 to 8.

4.3.4 Clamped uniformly loaded plate

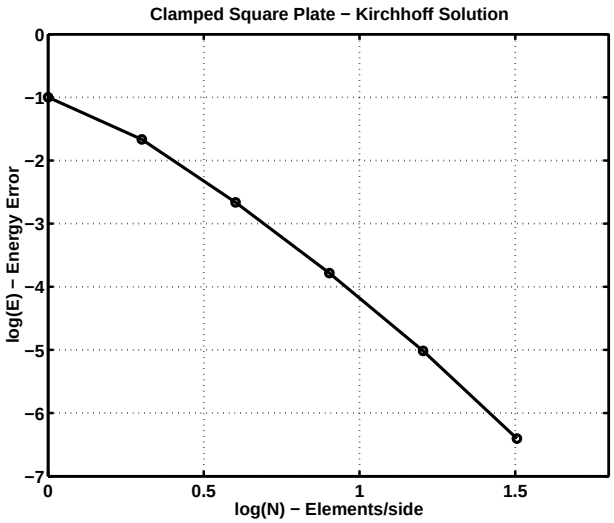

Figure 9: Energy error for square, uniformly loaded, clamped plate - No shear deformation

Accurate series solutions for clamped rectangular thin plates have been computed by Taylor & Govindjee [11] and are used to show the rate of convergence for the thin case in Fig. 9. General solutions for thick clamped plates are not available and in Fig. 10 we show the numerical behavior for the case of a square, uniformly loaded case.

4.3.5 Mirror of cubic material

In this example we consider the analysis of a mirror manufactured from a single crystal Silicon [111] wafer and loaded by a uniform pressure (0.01 $\mathrm{mN}/(\mu\mathrm{m})^2$) as shown in Fig. 11. The chosen orientation of the principal material axes leads to coupling between the membrane response and transverse

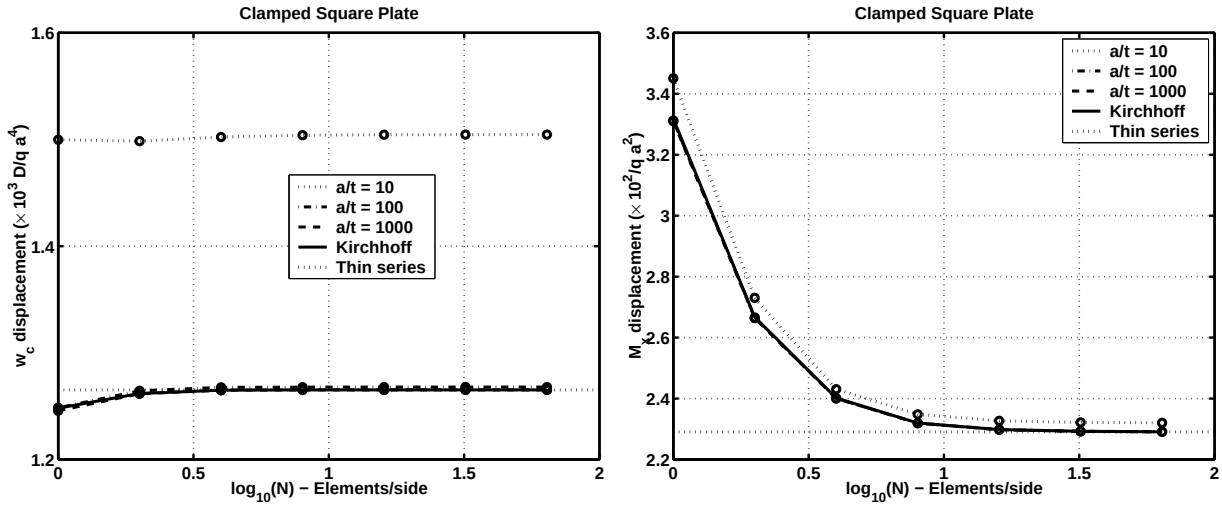

Figure 10: Center displacement and moment for square, uniformly loaded plate with clamped boundary conditions

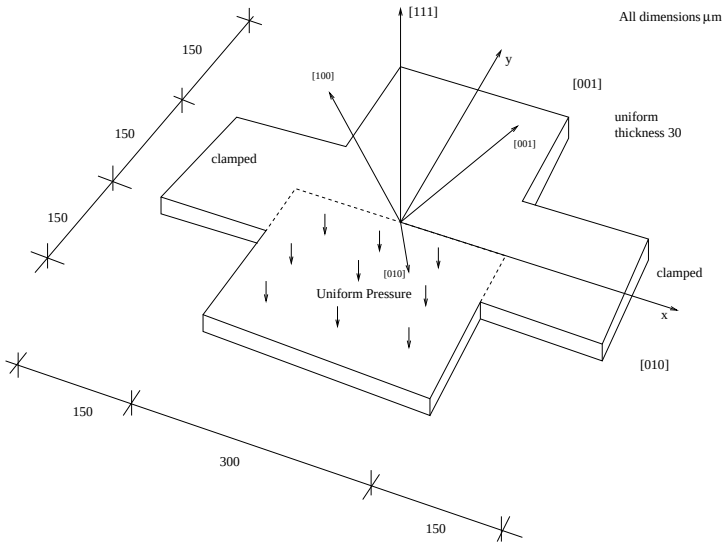

Figure 11: Geometry for mirror of cubic [111] material

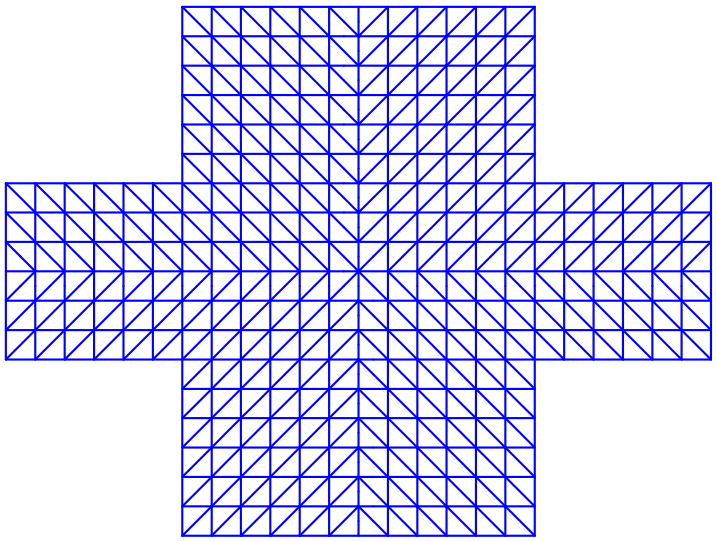

Figure 12: Typical finite element mesh for mirror of cubic [111] material

shear forces (see Appendix B). A mesh of 1,352 nodes and 576 elements with 93,355 degrees of freedom is shown in Fig. 12. We note that at the reentrant corner a singularity in solution variables exists and, consequently, optimal rates of convergence are not expected. Knowledge of the actual radius of curvature at the reentrant corner would permit modeling with a mesh which would produce the full rate of convergence. To illustrate this we show in Fig. 13 two dominant response quantities at the lower-left corner of the plate (viz. the transverse deflection and the fiber rotation about the x-axis) versus the number of degrees for freedom in the finite element model. There are two points of note: (1) the response of the plate is converging sub-optimally and (2) due to the mixed nature of the formulation the convergence is not guaranteed to be monotonic. In Fig. 14 we present contours for the displacement field in the plate and note that in addition to the transverse displacement w from the transverse load coupling effects lead to the non-zero in-plane displacements u and v.

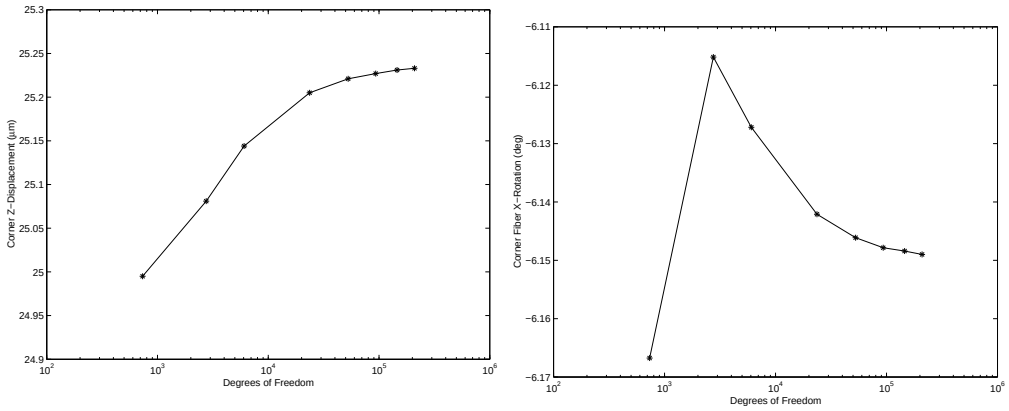

Figure 13: Lower-left corner response of anisotropic plate: (left) transverse deflection. (right) fiber x-rotation.

5 Closure

This report details the development of a 5-degree of freedom, 6-node triangular plate which combines a bending element with a membrane element. It is suitable for use in the simulation of anisotropic materials that generate membrane-shear coupling. In essence we have extended the plate element of Auricchio & Lovadina [7] to include membrane forces and anisotropic material behavior. The shear and the membrane force are treated as mixed in our treatment. Linking has been used so that the exact thin plate limit can be easily obtained, thus, the element can be used to analyze both thick and thin plate problems. Examples show the good properties of the development.

Acknowledgments

SG gratefully acknowledges the support of CITRIS through the SUGAR project.

References

[1] O.C. Zienkiewicz, Z. Xu, L.F. Zeng, A. Samuelsson, and N.-E. Wiberg. Linked interpolation for Reissner-Mindlin plate elements. Part I – a sim-

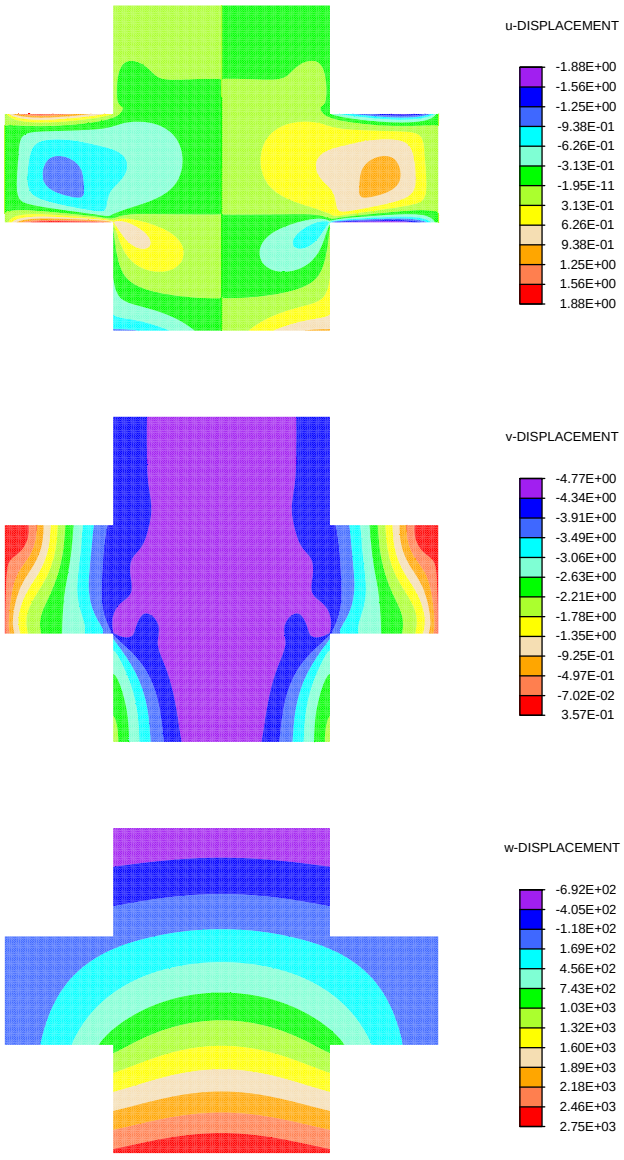

Figure 14: Displacement contours of anisotropic plate

ple quadrilateral element. *International Journal for Numerical Methods in Engineering*, 36:3043–3056, 1993.

[2] Z. Xu, O.C. Zienkiewicz, and L.F. Zeng. Linked interpolation for Reissner-Mindlin plate elements. Part III – an alternative quadrilateral. *International Journal for Numerical Methods in Engineering*, 36:3043–3056, 1993.

[3] R.L. Taylor and F. Auricchio. Linked interpolation for Reissner-Mindlin plate elements: Part II – a simple triangle. *International Journal for Numerical Methods in Engineering*, 36:3057–3066, 1993.

[4] F. Auricchio and R.L. Taylor. A shear deformable plate element with an exact thin limit. *Computer Methods in Applied Mechanics and Engineering*, 118:393–412, 1994.

[5] F. Auricchio and R.L. Taylor. A triangular thick plate finite element with an exact thin limit. *Finite Elements in Analysis and Design*, 19:57–68, 1995.

[6] O.C. Zienkiewicz and D. Lefebvre. Three field mixed approximation and the plate bending problem. *Comm. Appl. Num. Meth.*, 3:301–309, 1987.

[7] F. Auricchio and C. Lovadina. Analysis of kniematic linked interpolation methods for Reissner-Mindlin plate problems. *Computer Methods in Applied Mechanics and Engineering*, 190:2465–2482, 2001.

[8] C. Lovadina. Analysis of a mixed finite element for the Reissner-Mindlin plate problems. *Computer Methods in Applied Mechanics and Engineering*, 163:71–85, 1998.

[9] F. Brezzi, M. Fortin, and R. Stenberg. Error analysis of mixed-interpolated elements for Reissner-Mindlin plates. *Math. Models Methods Appl. Sci.*, 1:125–151, 1991.

[10] C. Chinosi and C. Lovadina. Numerical analysis of some mixed finite element methods for Reissner-Mindlin plates. *Computational Mechanics*, 16:36–44, 1995.

[11] R.L. Taylor and S. Govindjee. Solution of clamped rectangular plate problems. Technical Report UCB/SEMM-02/09, University of California, Berkeley, November 2002.

A Programming

The following groupings are made for the programming steps. The solution parameters are arranged as

$$\tilde{\mathbf{U}} = \begin{bmatrix} \tilde{\mathbf{v}}_i & \tilde{w}_b & \tilde{\mathbf{S}} & \tilde{\mathbf{R}} \end{bmatrix}$$

where

$$\tilde{\mathbf{v}}_i = \begin{bmatrix} \tilde{\mathbf{u}}_i \\ \tilde{\mathbf{w}}_i \end{bmatrix} \qquad \tilde{\mathbf{S}} = \begin{bmatrix} \tilde{\mathbf{N}} \\ \tilde{\mathbf{Q}} \end{bmatrix} \qquad \tilde{\mathbf{R}} = \begin{bmatrix} \tilde{\boldsymbol{\beta}} \\ \tilde{\phi}_b \end{bmatrix} \quad .$$

The stiffness matrix is arranged as

$$\mathbf{K} = \begin{bmatrix} \mathbf{A}_{vv} & \mathbf{0} & \mathbf{A}_{vs} & \mathbf{A}_{vb} \\ \mathbf{0} & 0 & \mathbf{A}_{ws} & \mathbf{0} \\ \mathbf{A}_{sv} & \mathbf{A}_{sw} & \mathbf{A}_{ss} & \mathbf{A}_{sb} \\ \mathbf{A}_{bv} & \mathbf{0} & \mathbf{A}_{bs} & \mathbf{A}_{bb} \end{bmatrix}$$

where

$$\mathbf{A}_{vv} = \begin{bmatrix} \mathbf{0} & \mathbf{0} \\ \mathbf{0} & \mathbf{A}_{ik}^{ww} \end{bmatrix}$$

$$\mathbf{A}_{ss} = \begin{bmatrix} \mathbf{H}_{jl}^{mm} & \mathbf{H}_{jl}^{ms} & \mathbf{H}_{j}^{mq} \\ \mathbf{H}_{jl}^{sm} & \mathbf{H}_{jl}^{ss} & \mathbf{H}_{j}^{sq} \\ \mathbf{H}_{l}^{qm} & \mathbf{H}_{l}^{qs} & H^{qq} \end{bmatrix} \qquad \mathbf{A}_{sv} = \begin{bmatrix} \mathbf{G}_{jk}^{mu} & \mathbf{0} \\ \mathbf{0} & \mathbf{G}_{jk}^{sw} \\ \mathbf{0} & \mathbf{G}_{k}^{qw} \end{bmatrix} = \mathbf{A}_{vs}^{T}$$

$$\mathbf{A}_{bb} = \begin{bmatrix} \mathbf{A}_{jl}^{\beta\beta} & \mathbf{A}_{j}^{\beta\phi} \\ \mathbf{A}_{l}^{\phi\beta} & A^{\phi\phi} \end{bmatrix} \qquad \mathbf{A}_{bs} = \begin{bmatrix} \mathbf{0} & \mathbf{G}_{jl}^{\beta s} & \mathbf{G}_{j}^{\beta q} \\ \mathbf{0} & \mathbf{G}_{l}^{\phi s} & G^{\phi q} \end{bmatrix} = \mathbf{A}_{sb}^{T}$$

$$\mathbf{A}_{bv} = \begin{bmatrix} \mathbf{0} & \mathbf{A}_{jk}^{\beta w} \\ \mathbf{0} & \mathbf{A}_{k}^{\phi w} \end{bmatrix} = \mathbf{A}_{vb}^{T} \qquad \mathbf{A}_{ws} = \begin{bmatrix} \mathbf{0} & \mathbf{G}_{l}^{bs} & G^{bq} \end{bmatrix} = \mathbf{A}_{sw}^{T} \quad .$$

Also the right hand side is grouped as

$$\mathbf{F} = \begin{bmatrix} \mathbf{F}_v & F_w & \mathbf{F}_s & \mathbf{F}_b \end{bmatrix}^T$$

where

$$\mathbf{F}_v = \begin{bmatrix} \mathbf{F}_i^u \\ \mathbf{F}_i^w \end{bmatrix} \qquad F_w = F_b^w \qquad \mathbf{F}_s = \begin{bmatrix} \mathbf{F}^N \\ \mathbf{F}^Q \end{bmatrix} \qquad \mathbf{F}_b = \begin{bmatrix} \mathbf{F}^\beta \\ F_b^\phi \end{bmatrix} \quad .$$

First eliminate the bubble modes

$$\bar{\mathbf{K}} = \begin{bmatrix} \bar{\mathbf{A}}_{vv} & \mathbf{0} & \bar{\mathbf{A}}_{vs} & \mathbf{0} \\ \mathbf{0} & 0 & \mathbf{A}_{ws} & \mathbf{0} \\ \bar{\mathbf{A}}_{sv} & \mathbf{A}_{sw} & \bar{\mathbf{A}}_{ss} & \mathbf{0} \\ \bar{\mathbf{A}}_{bv} & \mathbf{0} & \bar{\mathbf{A}}_{bs} & \mathbf{I} \end{bmatrix}$$

where

$$\begin{aligned} \bar{\mathbf{A}}_{vv} &= \mathbf{A}_{vv} - \mathbf{A}_{vb}\mathbf{A}_{bb}^{-1}\mathbf{A}_{bv} \\ \bar{\mathbf{A}}_{vs} &= \mathbf{A}_{vs} - \mathbf{A}_{vb}\mathbf{A}_{bb}^{-1}\mathbf{A}_{bs} = \bar{\mathbf{A}}_{sv}^{T} \\ \bar{\mathbf{A}}_{ss} &= \mathbf{A}_{ss} - \mathbf{A}_{sb}\mathbf{A}_{bb}^{-1}\mathbf{A}_{bs} \\ \bar{\mathbf{A}}_{bv} &= \mathbf{A}_{bb}^{-1}\mathbf{A}_{bv} \\ \bar{\mathbf{A}}_{bs} &= \mathbf{A}_{bb}^{-1}\mathbf{A}_{bs} \end{aligned}$$

and likewise the force becomes

$$\bar{\mathbf{F}} = \begin{bmatrix} \bar{\mathbf{F}}_v & F_w & \bar{\mathbf{F}}_s & \bar{\mathbf{F}}_b \end{bmatrix}^T$$

where

$$\begin{aligned} \bar{\mathbf{F}}_v &= \mathbf{F}_v - \mathbf{A}_{vb}\mathbf{A}_{bb}^{-1}\mathbf{F}_b \\ \bar{\mathbf{F}}_s &= \mathbf{F}_s - \mathbf{A}_{sb}\mathbf{A}_{bb}^{-1}\mathbf{F}_b \\ \bar{\mathbf{F}}_b &= \mathbf{A}_{bb}^{-1}\mathbf{F}_b \quad . \end{aligned}$$

Next eliminate the shear modes

$$\hat{\mathbf{K}} = \begin{bmatrix} \hat{\mathbf{A}}_{vv} & \hat{\mathbf{A}}_{vw} & \mathbf{0} & \mathbf{0} \\ \hat{\mathbf{A}}_{wv} & \hat{A}_{ww} & \mathbf{0} & \mathbf{0} \\ \hat{\mathbf{A}}_{sv} & \hat{\mathbf{A}}_{sw} & \mathbf{I} & \mathbf{0} \\ \bar{\mathbf{A}}_{bv} & \mathbf{0} & \bar{\mathbf{A}}_{bs} & \mathbf{I} \end{bmatrix}$$

where

$$\begin{aligned} \hat{\mathbf{A}}_{vv} &= \bar{\mathbf{A}}_{vv} - \bar{\mathbf{A}}_{vs}\bar{\mathbf{A}}_{ss}^{-1}\bar{\mathbf{A}}_{sv} \\ \hat{\mathbf{A}}_{vw} &= -\bar{\mathbf{A}}_{vs}\bar{\mathbf{A}}_{ss}^{-1}\mathbf{A}_{sw} = \hat{\mathbf{A}}_{wv}^{T} \\ \hat{A}_{ww} &= -\mathbf{A}_{ws}\bar{\mathbf{A}}_{ss}^{-1}\mathbf{A}_{sw} \\ \hat{\mathbf{A}}_{sv} &= \bar{\mathbf{A}}_{ss}^{-1}\bar{\mathbf{A}}_{sv} \\ \hat{\mathbf{A}}_{sw} &= \bar{\mathbf{A}}_{ss}^{-1}\mathbf{A}_{sw} \end{aligned}$$

and again the force becomes

$$\hat{\mathbf{F}} = \left[\begin{array}{cccc} \hat{\mathbf{F}}_v & \hat{F}_w & \hat{\mathbf{F}}_s & \bar{\mathbf{F}}_b \end{array} \right]^T$$

where

$$\begin{aligned} \hat{\mathbf{F}}_v &= \bar{\mathbf{F}}_v - \bar{\mathbf{A}}_{vs}\bar{\mathbf{A}}_{ss}^{-1}\bar{\mathbf{F}}_s \\ \hat{F}_w &= F_w - \bar{\mathbf{A}}_{ws}\bar{\mathbf{A}}_{ss}^{-1}\bar{\mathbf{F}}_s \\ \hat{\mathbf{F}}_s &= \bar{\mathbf{A}}_{ss}^{-1}\bar{\mathbf{F}}_s \quad . \end{aligned}$$

Finally, eliminate the bubble displacement mode to yield the final element stiffness and force arrays as

$$\tilde{\mathbf{K}}\,\tilde{\mathbf{U}} = \left[\begin{array}{cccc} \mathbf{K}_{vv} & \mathbf{0} & \mathbf{0} & \mathbf{0} \\ \tilde{\mathbf{A}}_{wv} & 1 & \mathbf{0} & \mathbf{0} \\ \hat{\mathbf{A}}_{sv} & \hat{\mathbf{A}}_{sw} & \mathbf{I} & \mathbf{0} \\ \bar{\mathbf{A}}_{bv} & \mathbf{0} & \bar{\mathbf{A}}_{bs} & \mathbf{I} \end{array} \right] \left[\begin{array}{c} \tilde{\mathbf{v}} \\ \tilde{w}_b \\ \tilde{\mathbf{S}} \\ \tilde{\mathbf{R}} \end{array} \right] = \left[\begin{array}{c} \mathbf{P}_v \\ \tilde{F}_w \\ \hat{\mathbf{F}}_s \\ \bar{\mathbf{F}}_b \end{array} \right]$$

where

$$\begin{aligned} \mathbf{K}_{vv} &= \hat{\mathbf{A}}_{vv} - \hat{\mathbf{A}}_{vw}\hat{A}_{ww}^{-1}\hat{\mathbf{A}}_{wv} \\ \mathbf{P}_v &= \hat{\mathbf{F}}_v - \hat{\mathbf{A}}_{vw}\hat{A}_{ww}^{-1}\hat{F}_w \\ \tilde{\mathbf{A}}_{wv} &= \hat{A}_{ww}^{-1}\hat{\mathbf{A}}_{wv} \\ \tilde{F}_w &= \hat{A}_{ww}^{-1}\hat{F}_w \quad . \end{aligned}$$

B Couplings in single crystal Silicon

In MEMS design single crystal Silicon is often used in the construction of devices. This is an anisotropic material with cubic symmetry. Typical wafers are either [100] or [111]. Thus, plate structures are fabricated where the plate thickness in either oriented in a [100] crystal direction or a [111] crystal direction. To assess the importance of the material anisotropy on the response of plate structures we can plot the moduli giving rise to $\mathbf{D}_{bb}$, $\mathbf{D}_{mm}$, $\mathbf{D}_{ms}$, and $\mathbf{D}_{ss}$ as a function of angle between the coordinate system of the device and the crystal axes. The wafer geometries to be considered are shown in Figure 15. For each wafer we show the crystallographic axes of the underlying Silicon lattice and we also show an angle β that orients an (x_1, x_2, x_3) coordinate system of the device.

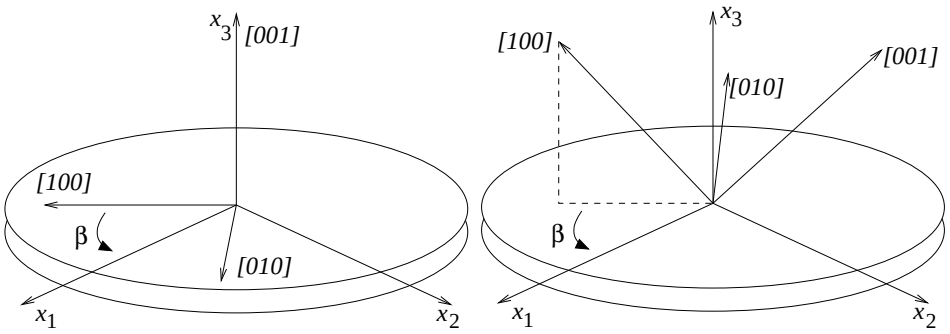

Figure 15: Wafer geometries; (100) wafer right and (111) wafer left.

Shown in Fig. 16 for a [100] wafer and in Fig. 17 for a [111] wafer are the relevant moduli that determine the anisotropic response of the plate. One can note the following important features of the material response.

1. For single crystal Si plates structures fabricated from [100] wafers:
   (a) The membrane and the bending response will depend upon the orientation of the plate.
   (b) There is a bending-twisting coupling.
   (c) There is no membrane-shear coupling.
   (d) The through thickness shear response is isotropic in the plane.
2. For single crystal Si plates structures fabricated from [111] wafers:
   (a) The membrane and the bending response will be isotropic in the plane.
   (b) There is no bending-twisting coupling.
   (c) There is a membrane-shear coupling.
   (d) The through thickness shear response is isotropic in the plane.

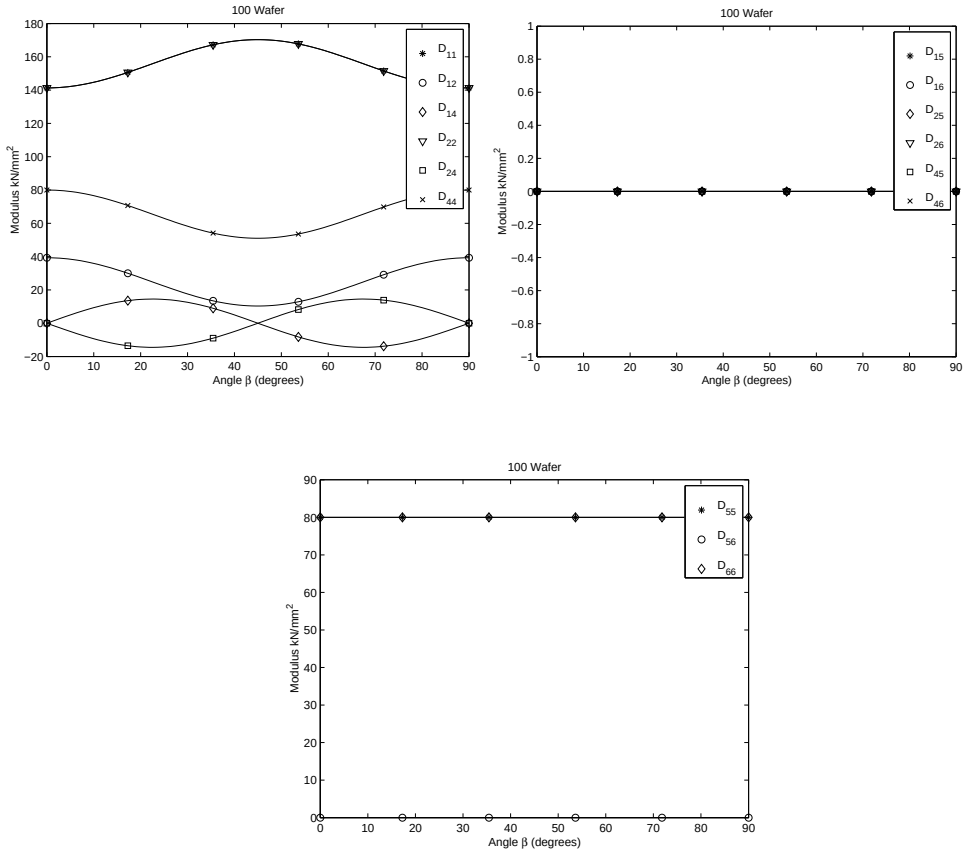

Figure 16: Reduced plane stress moduli for single crystal Silicon in [100] wafers. Upper left gives bending and membrane response. Upper right gives membrane shear coupling. Lower center gives through thickness shear response. (Angle β is as defined in Fig. 15.)

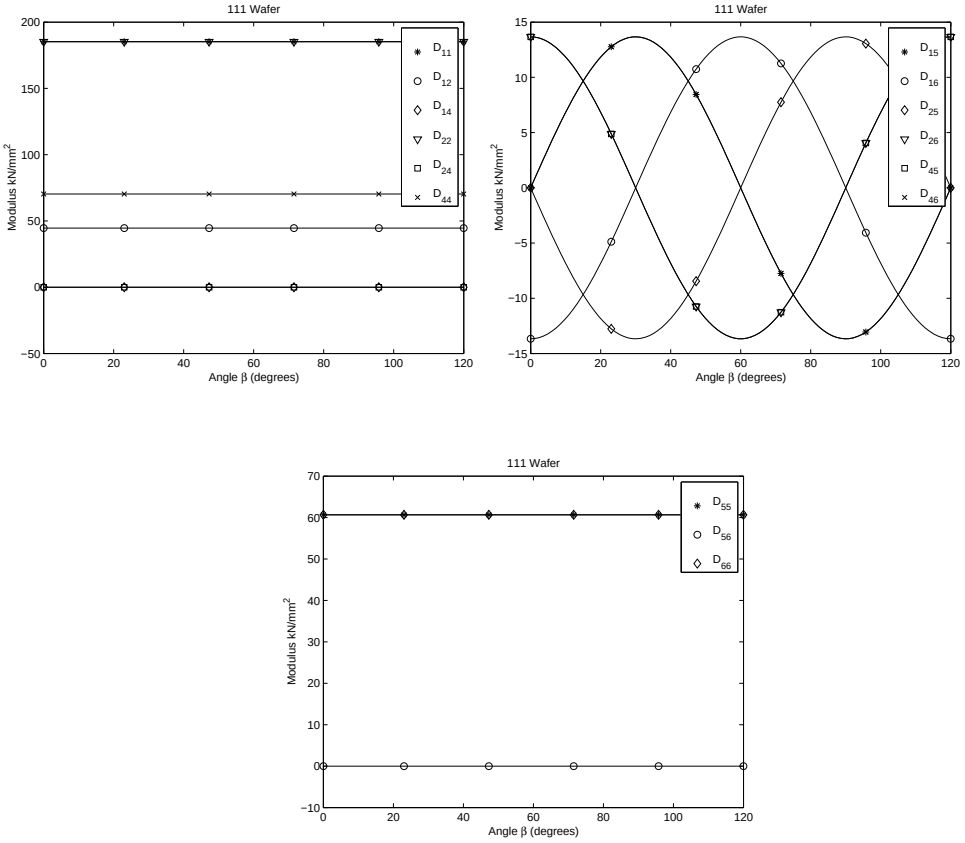

Figure 17: Reduced plane stress moduli for single crystal Silicon in [111] wafers. Upper left gives bending and membrane response. Upper right gives membrane shear coupling. Lower center gives through thickness shear response. (Angle β is as defined in Fig. 15.)